Joint EPRI – 123HiMAT International Conference on
Advances in High Temperature Materials
October 21–24, 2019, Nagasaki, Japan
J. Shingledecker, M. Takeyama, editors
https://doi.org/10.31339/asm.cp.am-epri-2019p1048

EVALUATION OF WELD CRACKING SUSCEPTIBILITY OF CANDIDATE NI-BASED ALLOYS FOR ADVANCED USC BOILERS

Nobuhiko Saito, Nobuyoshi Komai, Keita Hashimoto
Mitsubishi Heavy Industries, Ltd., Nagasaki, Japan

Masaki Kitamura
Mitsubishi Hitachi Power Systems, Ltd., Kanagawa, Japan

ABSTRACT

The susceptibilities of hot cracking and reheat cracking of A-USC candidate Ni-based alloys were evaluated relatively by Trans-Varestraint testing and Slow Strain Rate Tensile (SSRT) testing. In addition, semi-quantitative evaluation of the stress relaxation cracking susceptibility of Alloy 617 was conducted, because stress relaxation cracking in the heat affected zone (HAZ) has actually been reported for repair welds in Alloy 617 steam piping in European A-USC field-testing. Solidification cracking susceptibilities of Alloy 617 were the highest; followed by HR35, Alloy 740 and Alloy 141, which were all high; and then by HR6W and Alloy 263, which were relatively low. In addition, liquation cracking was observed in the HAZ of Alloy 617. The reheat cracking susceptibilities of Alloy 617, Alloy 263, Alloy 740 and Alloy 141 were somewhat higher than those of HR6W and HR35 which have good creep ductility due to the absence of γ' phase precipitates. A method to evaluate stress relaxation cracking susceptibility was developed by applying a three-point bending test using a specimen with a V-notch and finite element analysis (FEA), and it was shown that stress relaxation cracking of aged Alloy 617 can be experimentally replicated. It was proposed that a larger magnitude of creep strain occurs via stress relaxation during the three-point bending test due to a higher yield strength caused by γ' phase strengthening, and that low ductility due to grain boundary carbides promoted stress relaxation cracking. The critical creep strain curve of cracking can be created by means of the relationship between the initial strain and the creep strain during the three-point bending tests, which were calculated by FEA. Therefore, the critical conditions to cause cracking could be estimated from the stress relaxation cracking boundary from of the relationship between the initial strain and the creep strain during the three-point bending test.

Keywords: A-USC, Ni-based alloy, weld cracking, stress relaxation cracking, Three-point bending test

INTRODUCTION

Ni-based alloys, which are much stronger in creep than conventional heat resistant steel currently used in 600°C class USC power plants, are candidate alloys for boiler components exposed to 700°C class steam conditions. It is well known that candidate Ni-based alloys may be susceptible to a host of weldability issues such as solidification cracking, heat affected zone liquation cracking, ductility dip cracking, strain age cracking and stress relief cracking (also known as stress relaxation cracking) [1, 2]. In particular, Ni-based alloys may have a relatively high susceptibility to strain age cracking and stress relaxation cracking in welds. Strain age cracking and stress relaxation cracking are solid state cracking phenomena that are most often observed in the coarse-grained heat affected zone (CGHAZ) adjacent to the fusion boundary, although it is possible for such cracking to occur in the weld metal of these alloys. These cracks are always

intergranular. Although stress relaxation cracking occurs in the short term of reheating in service or post weld heat treatment (PWHT), strain age cracking also occurs in the longer term at service-relevant temperatures and stresses. Stress relaxation cracking in the HAZ has actually been reported in repair welds of Alloy 617 steam piping in European A-USC field-testing [2]. Given this fact, in the case of repair welding of the pipe, there is concern that stress relaxation cracking may occur during high temperature service exposure. Many testing methodologies have been developed to understand stress relaxation cracking. Still, the underlying mechanism has yet to be determined. This is mainly due to the lack of a holistic testing methodology that can give a definitive evaluation of cracking susceptibility [1]. In this study, therefore, semi-quantitative evaluation of the stress relaxation cracking susceptibility of Alloy 617, which is a candidate material for steam piping in Japan, was conducted. In addition, susceptibilities of hot cracking and reheat cracking of candidate Ni-based alloys were evaluated relatively by Trans-Varestraint [3] testing and SSRT testing [4], respectively.

TEST MATERIALS

The plate materials HR6W, HR35, Alloy 617, Alloy 263, Alloy 740 and Alloy 141, which are candidate materials for A-USC boilers in Japan [5], were used in the evaluation of susceptibility of hot cracking and reheat cracking. Table 1 shows the chemical composition and the solution heat treatment conditions. The ingots were melted by the Vacuum Induction Melting (VIM) process and then forged and hot rolled to a thickness of 25 mm. After forging, the solution annealing was carried out under the respective conditions shown in Table 1.

Table 1 Chemical composition and solution annealing conditions of Ni-based alloy plate

Material	Chemical composition (mass%)														Solution annealing
	C	Si	Mn	P	S	Ni	Cr	Mo	Ti	Nb	B	W	Co	Sol.Al	
HR6W	0.082	0.22	1.03	0.011	<0.001	45.31	23.07	-	0.10	0.20	0.0042	7.07	-	-	1220°C × 1h
HR35	0.083	0.12	0.12	0.002	<0.001	50.34	29.77	-	0.83	-	0.0040	4.03	-	-	1230°C × 1h
Alloy 617	0.070	0.12	0.11	0.005	<0.001	bal.	22.02	8.95	0.41	-	0.0044	-	11.75	1.27	1175°C × 1h
Alloy 263	0.064	0.11	0.11	0.005	<0.001	bal.	20.19	5.90	2.22	-	0.0040	-	19.99	0.48	1150°C × 1h
Alloy 740	0.033	0.12	0.11	0.007	<0.001	bal.	25.11	0.54	1.87	2.01	0.0040	-	20.06	0.93	1150°C × 1h
Alloy 141	0.031	0.11	0.11	0.006	<0.001	bal.	20.18	9.92	1.67	-	0.0049	-	-	1.24	1066°C × 1h

In order to evaluate the effect of material conditions on the stress relaxation cracking susceptibility of Alloy 617, solution-annealed materials and materials aged for 3000 hours at 700°C of Alloy 617 plate were prepared. Furthermore, additional heat treatment simulating coarse-grained HAZ at 1300°C for 5 seconds was applied using the following procedure. First an electric furnace was heated to 1300°C. Specimens attached with a thermocouple were then quickly placed in the furnace, reheated to 1300°C, and held for 5 seconds. They were then taken out of the furnace and cooled to room temperature by being quenched in water. The process from placing the specimens in the furnace to removing them took about 5 minutes.

EXPERIMENTAL PROCEDURE

Susceptibility of candidate A-USC alloys to hot cracking

Plate specimens of 4mm in thickness, 100mm in width and 100mm in length were prepared by machining. Trans-Varestraint testing applies strain by forcing a plate to bend during non-filler welding on the plate surface. It then evaluates susceptibility to hot cracking based on the crack

length. Test conditions are shown in Table 2. The applied strain was 3%. After the test, the maximum crack length and total crack length at the weld bead center were measured, and the relative evaluation of hot (solidification) cracking susceptibility between candidate alloys was carried out. In addition, the cross-sectional optical microstructure of the bead center was observed. As a result of the observation, liquation cracking was confirmed in the HAZ under the bead of some alloys. Therefore, the maximum crack length and total crack length of the HAZ in the same section were also measured.

Table 2 Test conditions of Trans-Varestraint testing

Welding method	Electric current (A)	Voltage (V)	Welding speed (mm/min.)	Ar gas shielding (L/min.)	Applied strain (%)
GTAW (Non Filler)	100	12-13	150	10	3

Susceptibility of candidate A-USC alloys to reheat cracking

Since reheat cracking generally occurs in the CGHAZ adjacent to the fusion boundary, the simulated CGHAZ of each candidate material was prepared. Round bar specimens with diameter of 16mm were heated to 1300°C (equivalent to the maximum attainable temperature in the CGHAZ) in about 70 seconds by means of high frequency induction heating, held for 5 seconds, and then cooled down to 300°C in about 80 seconds. After that, test specimens with diameters of 7mm in the parallel portion were produced by machining. SSRT testing was conducted at 700°C, 750°C and 800°C to confirm the temperature dependence of reheat cracking susceptibility. The crosshead speed was 0.5mm/minute (gauge length: 25mm), and the susceptibility to reheat cracking between candidate alloys was evaluated relatively by the reduction in area of specimens after the test.

Stress relaxation tests were carried out to confirm the effectiveness of post weld heat treatment for reheat cracking. Test specimens 10 mm in diameter were processed from the simulated CGHAZ alloys. The test temperatures were 700°C, 900°C and 980°C [6], which are considered to be the post weld heat treatment temperatures of Alloy 617B in Europe. The stress relaxation behavior was evaluated by heating for 20h under a strain of 1% and that strain was kept constant within a gauge length of 15mm. Test specimens were heated to the target temperature by means of high frequency induction heating, and stress relaxation testing was conducted by a fatigue testing machine (Shimadzu servopulser, capacity: 100 kN).

Susceptibility of Alloy 617 to stress relaxation cracking

Three-point bending test

A three-point bending test was applied to evaluate stress relaxation cracking susceptibility. This test method simulates similar stress relaxation behavior in actual plants, and the control of both stress and strain is straightforward. The three-point bending test specimen used in this work is shown in Fig.1. A V-notch was placed along the longitudinal center of the specimen. In the COMTES700 project in Europe, although a three-point bending test method was applied in the evaluation of relaxation cracking [6], a specimen without a notch was used. By placing a V-notch in test specimen, the stress relaxation rate around the notch root can be reduced by means of high restriction conditions. The specimen was placed in a bending fixture equipped with a screw hole as shown in Fig.2. An SUS304 plate was used to make the bending fixture and the screw. In order to avoid creep deformation during the three-point bending test at 700°C, the bending fixture was made sufficiently thick as compared with the test specimen. By tightening the screw, an equivalent strain (initial strain) is applied, which is the sum of the elastic strain and plastic strain. The tightening length was determined by finite element analysis (FEA) results of the relationship between the equivalent strain and the tightening length. In order to set initial strains of 1%, 3%,

5%, 8%, 10%, and 15%, the tightening length of the screw was set to 0.29 mm, 0.51 mm, 0.67 mm, 0.91 mm, 1.08 mm and 1.50 mm respectively. The FEA method and material properties used in the analysis will be described later. Each specimen was heated to 700°C in an electric furnace. After 1, 3, 10, 30, 100 and 300 hours of heating, normal contrast (red-white) penetrant testing (PT) of the notch root was performed to detect the presence of cracks. After testing, selected specimens were sectioned at the center of the crack length, mounted in epoxy, and polished using standard metallographic techniques. These specimens were used for optical microscopy (OM) and were etched using a solution of 25% HNO_3 and 75% HCl. Scanning electron microscopy (SEM) was performed on polished unetched samples in both the secondary (SE) and back-scatter (BSE) electron imaging modes. Energy dispersive spectroscopy (EDS) mapping was conducted for the estimation of precipitation. Then transmission electron microscopy (TEM) was conducted on as-solution-annealed and as-aged plate materials in order to evaluate the fine precipitation state in the grain. Vickers hardness in the grains before and after the three-point bending test near the edge of specimens was measured at a load of 200g.

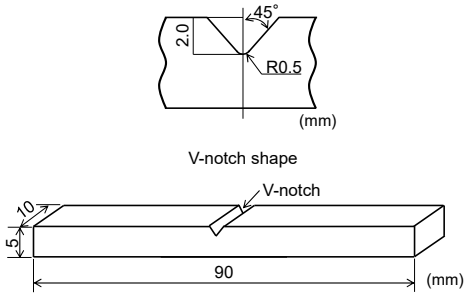

Figure 1 Three-point bending test specimen

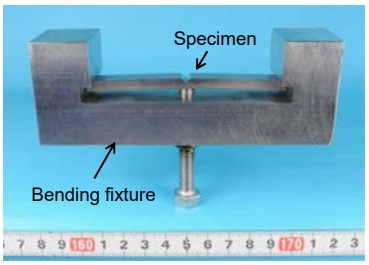

Figure 2 Appearance of three-point bending test specimen

Computational thermodynamics

Equilibrium thermodynamic calculations for equilibrium phase fractions of plate material were conducted using the commercial code of JMatPro version 8.0 using the database of Ni-based alloys [7]. The volume fraction changes of the γ' phase during long-term aging at 700°C, 750°C and 800°C were also calculated in order to discuss the results of the three-point bending test.

Finite element analysis method

Finite element analysis (FEA) was conducted using ABAQUS version 6.10 in order to confirm the relationship between the initial strain at the notch root and the tightening length of the screw, and the relationship between the initial strain and the creep strain during the three-point bending test. The strain was calculated by the Mises equivalent strain expressed by Equation (1).

$$\varepsilon_{eq} = \frac{\sqrt{2}}{2(1+\nu)}\sqrt{\left(\varepsilon_x - \varepsilon_y\right)^2 + \left(\varepsilon_y - \varepsilon_z\right)^2 + (\varepsilon_z - \varepsilon_x)^2 + 3/2\left({\gamma_{xy}}^2 + {\gamma_{yz}}^2 + {\gamma_{zx}}^2\right)} \qquad (1)$$

where, ε_{eq} is equivalent strain, ν is Poisson's ratio, $(\varepsilon_x, \varepsilon_y, \varepsilon_z)$ is strain in the x, y, z directions, and $\left(\gamma_{xy}, \gamma_{yz}, \gamma_{zx}\right)$ is shear strain in each direction

A quarter model of the three-point bending test specimen used for FEA is shown in Fig.3. The minimum element size of the notch root was 0.05mm, and the strain of the node was used for evaluation. First, an elastic-plastic analysis was carried out at room temperature (25°C) to determine the tightening length of the screw. Subsequently, the creep strain generated in the stress relaxation process was calculated by elastic-plastic creep analysis under displacement restraint.

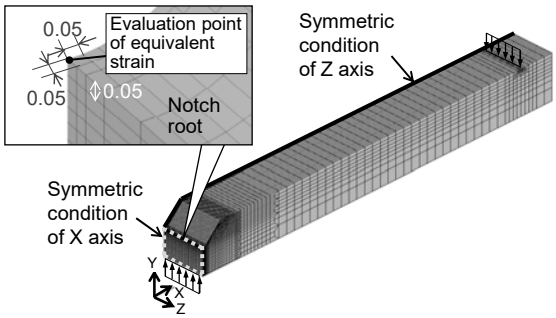

Figure 3 Quarter model of three-point bending test specimen for finite element analysis

The stress-strain curves of solution-annealed material and aged material using FEA are shown in Fig.4. Young's modulus and the linear expansion coefficient for Alloy 617 were taken from data in literature [8]. The minimum creep rate at 700°C used in FEA is expressed by Equation (2) which was obtained from the relationship between Larson-Miller parameter plots and the minimum creep rate as a function of the stress for Alloy 617 [8]. In this case, the creep and relaxation of the screw and the fixture were not considered.

$$\dot{\varepsilon}_c = 2.417 \times 10^{-28} \cdot \sigma^{9.074} \qquad (2)$$

where, $\dot{\varepsilon}_c$ is minimum creep rate in %/h, and σ is stress in MPa.

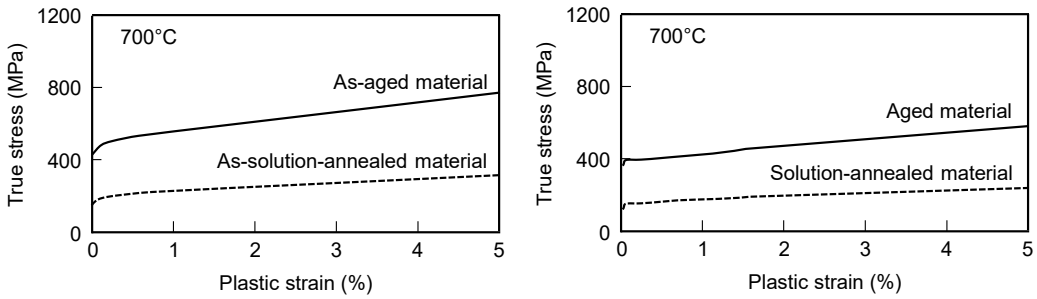

(a) No simulated HAZ heat treatment *(b) After simulated HAZ heat treatment*

Figure 4 High temperature tensile properties at 700℃ of tested material

RESULTS AND DISCUSSION

Susceptibility of candidate A-USC alloys to hot cracking

The appearance of cracks in the weld bead of Alloy 617 plate and the cross-sectional optical microstructure of the weld bead tip after Trans-Varestraint testing are shown in Fig.5. The cracks propagated at the dendritic boundary, indicating that these cracks are caused by solidification cracking. In some alloys, intergranular cracking was observed in the CGHAZ just below the weld bead. These cracks are caused by liquation cracking, which can be seen from the fact that the position where the crack occurs is in the vicinity of the fusion part and the shape of the crack tip is rounded.

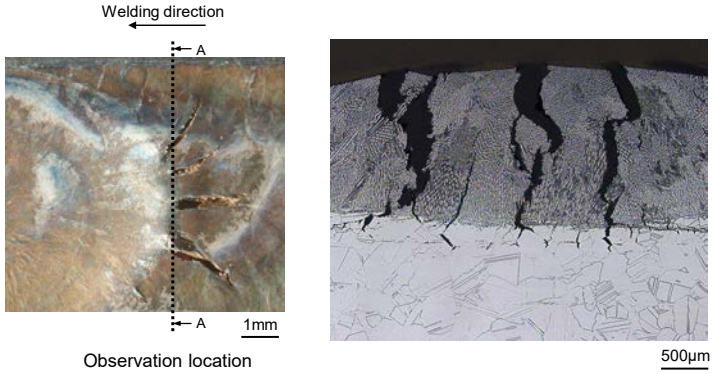

Figure 5 Occurrences and cross section optical microstructure of Alloy 617 plate

Figure 6 shows the measurement results of the maximum crack length and total crack length generated in the solidification zone. The total crack length which is equal to the sum of all crack lengths of Alloy 617 was the longest in relative order, followed by HR35, Alloy 740, Alloy 141, HR6W, and Alloy 263. Crack length is correlated with susceptibility to solidification cracking. Alloy 617, which has the longest crack length, is considered to be more susceptible to solidification cracking, while HR6W and Alloy 263, which have shorter crack lengths, are considered to be relatively less susceptible to cracking. Figure 7 shows the measurement results of the maximum crack length and the total crack length generated in the CGHAZ. Cracks were observed in HR6W, HR35, Alloy 617 and Alloy 141, but the total crack length of Alloy 617 was the longest. Since the length of cracks in the HAZ is correlated with the susceptibility to liquation cracking, Alloy 617 is considered to have a high susceptibility to liquation cracking. The effect of high contents of phosphorus, sulfur and boron on hot cracking has been reported [9, 10]. In the Alloy 617 tested, the amount of phosphorus and sulfur was smaller and the amount of boron slightly larger than in other alloys. On the other hand, Alloy 141 has the highest boron content, but the crack length of Alloy 141 is almost the same as that of the alloys other than Alloy 617. Therefore, the reason Alloy 617 is susceptible to hot cracking cannot be explained by boron content alone. Therefore, it is necessary to clarify the reason why Alloy 617 is susceptible to hot cracking by confirming the influence of other impurities and the state of the formation of impurities such as boron on grain boundaries.

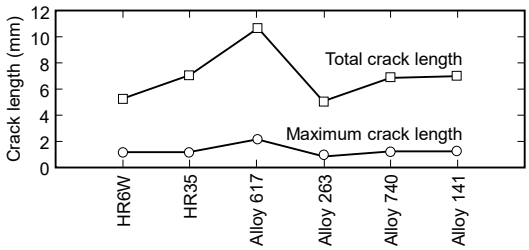

Figure 6 Trans-Varestraint test results for candidate A-USC alloys in solidification zone

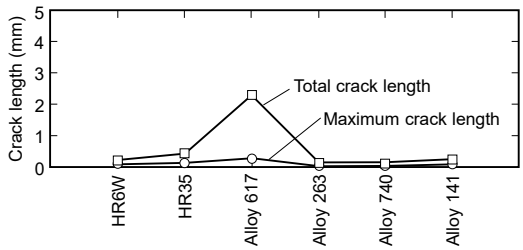

Figure 7 Trans-Varestraint test results for candidate A-USC alloys in CGHAZ

Susceptibility of candidate A-USC alloys to reheat cracking

Figure 8 shows the SSRT testing results of candidate A-USC alloys. The reduction of area (ROA) is small in Alloy 263, Alloy 740 and Alloy 141, and large in HR6W and HR35. In the former group, the ROA decreases as the test temperature increases, while in the latter group, the ROA increases as the test temperature increases. On the other hand, Alloy 617 has a small ROA at 700°C, but has a ROA equivalent to HR6W and HR35 at 750°C and 800°C. The ROA is correlated with reheat cracking susceptibility, therefore Alloy 263, Alloy 740 and Alloy 141 with

small ROA are considered to have high susceptibility to reheat cracking. Since these alloys are γ' strengthened alloys, it is considered that a large amount of the γ' phase reduces the fracture ductility and increases reheat cracking susceptibility. In the test temperature range, the equilibrium γ' phase fraction is slightly smaller at higher temperatures, but since the γ' phase precipitates earlier at higher temperatures it is considered that the fracture ductility is smaller. Alloy 617 tends to recover fracture ductility at 800°C, which is considered to be due to the small equilibrium γ' phase fraction at this temperature and the solid solution of the γ' phase in the matrix [11]. Since HR6W and HR35 are alloys having no precipitation in the γ' phase and being strengthened by other precipitation phases (Laves phase or α-Cr phase) [11], it is considered that the difference of strength between the in-grain and grain boundaries is smaller and the fracture ductility is higher than that of the γ' strengthened alloys. From the above results, it is clear that the γ' phase strengthened alloys have high reheat cracking susceptibility. Therefore, when these alloys are used in heavy thickness and large diameter pipes, it is necessary to perform post weld heat treatment such as re-solution annealed treatment or stress relief annealing from the viewpoint of preventing reheat cracking.

Figure 9 shows the stress relaxation test results of candidate A-USC alloys at 700°C, 900°C and 980°C. As a result of the test at 700°C, the stress of HR6W and HR35 decreased to 100 MPa or less when held for about 5 hours, but the stress relaxation amount of the other alloys is small, and the stress after being held for 20 hours is 200 MPa or more. Considering that HR6W and HR35 are alloys in which the γ' phase is not precipitated, the stress relaxation amount is considered to be correlated with the phase fraction of the γ' phase. On the other hand, at 900°C, the amount of stress relaxation increases in all of the alloys, and the stress is relaxed to 100 MPa or less after being held for 20 hours. This is caused by a decrease in the volume fraction of the γ' phase. The stress relaxation amounts of Alloy 141 and Alloy 740 that have large volume fractions of the γ' phase tend to be smaller than those of other alloys. It has been confirmed that stress is remarkably relaxed in all alloys at 980°C. From the above results, it is considered that the post welding heat treatment of candidate A-USC alloys should be 900°C or higher from the viewpoint of stress relaxation. Furthermore, it is considered desirable that alloys with large volume fractions of the γ' phase such as Alloy 740 and Alloy 141 are subjected to heat treatment at 980°C or higher.

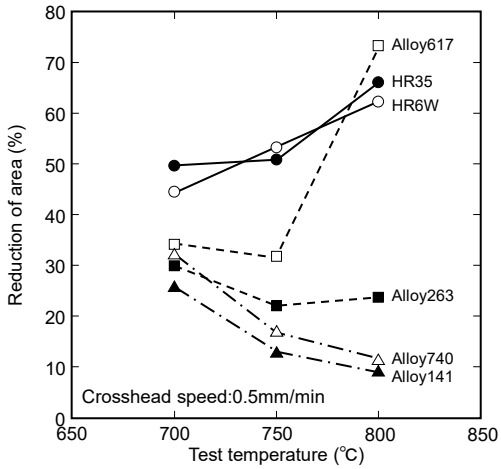

Figure 8 Slow Strain Rate Tensile test results of candidate A-USC alloys

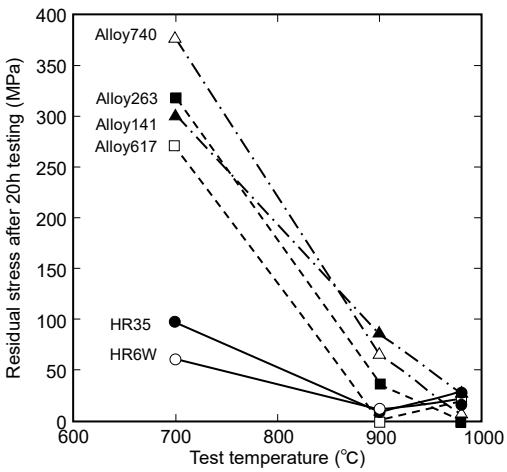

Figure 9 Stress relaxation test results of candidate A-USC alloys

Susceptibility of Alloy 617 to stress relaxation cracking

Three-point bending test results

Cracking was observed only in as-aged materials, while conversely, no cracks were found in specimens of the other materials. Figure 10 shows the heating time and initial strain diagram demonstrating the occurrence or absence of cracking in as-aged material. In as-aged material without simulated HAZ heat-treatment, specimens initially strained by 3%, 5%, 8% and 10% exhibited PT defect indication after 508, 30, 3 and 3 hours of heating, respectively. Only the specimen initially strained by 3% was intact with no cracking detected or visually observed after 300 hours. The time-to-crack tends to be shorter with increased initial strain. Figure 11 shows PT results and the cross-sectional optical microstructure at the notch root of 5% and 10% initially strained materials. Typical stress relaxation cracking characterized by intergranular cracks was seen in both samples. According to the three-point bending test results without a notch in the COMTES700 project, relaxation cracking of 10% initially strained Alloy 617 was noted under 700°C - operating condition in actual power plant after 10 hours of heating [6]. The test results from the COMTES700 project are almost the same as our test results for 10% initially strained specimens, which showed that the cracks occurred during 1 to 3 hours of heating. The reason why the time-to-crack in our test result was shorter than that of COMTES700's test result may be due to differences in the specimen's geometry (i.e. notched bar).

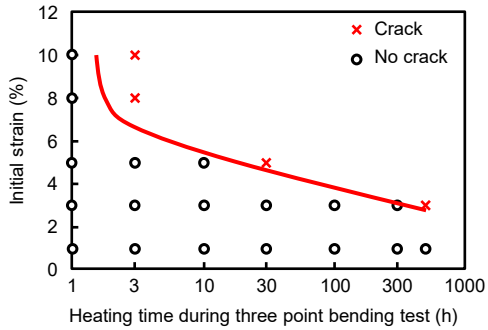

Figure 10 Heating time and initial strain diagram demonstrating the occurrence or absence for the as-aged material

Initial strain	5%	10%
Time to crack	30h	3h
Penetrant test results	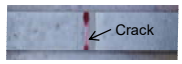	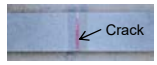
Optical microstructure at notch root	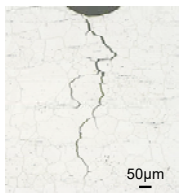	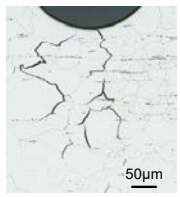

Figure 11 Penetrant test results and optical microstructure at notch root after three-point bending test of as-aged Alloy 617

Effect of precipitation on stress relaxation cracking susceptibility

Figure 12 shows SE images comparing as-solution-annealed specimens, as-aged specimens and simulated HAZ specimens of aged materials before and after three-point bending tests for various times. Precipitates in the grains and at the grain boundaries were not observed in as-solution-annealed materials before the test and after 3 hours of testing at 700°C; however grain boundary precipitates were observed after 300 hours of testing. Grain boundary precipitates were assumed to be $M_{23}C_6$ carbides since Cr, Mo and C were confirmed to be the main elements present by EDS analysis. In the aged materials, fine precipitates in the grains and $M_{23}C_6$ carbides at the grain boundary were observed in the specimen before testing. The precipitation state of aged materials after 3 hours and 508 hours of testing at 700°C were also the same. In the simulated HAZ materials of aged materials, a small number of $M_{23}C_6$ carbides were observed at the grain boundary; however precipitates in the grain were not found. This is presumed to be due to a solid solution of precipitates in the matrix by the heat treatment simulating coarse-grained HAZ. Although the precipitation state in the specimen after 3 hours of testing was almost the same as that of the specimen before the test, a coarsening tendency of precipitates was confirmed in the specimens after 300 hours of testing. There was no significant difference in the grain boundary precipitates after 300 hours and 508 hours of testing regardless of the type of test material.

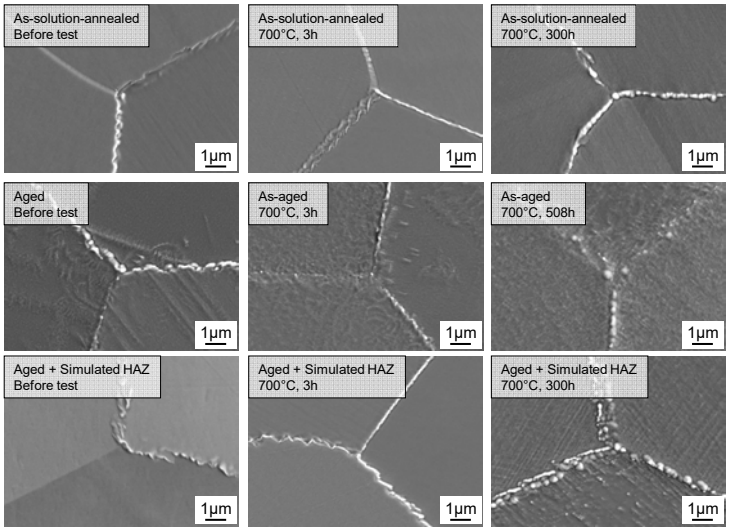

Figure 12 SE images comparing as-solution-annealed specimens, as-aged specimens and simulaed HAZ specimens of aged materials before and after three-point bending testing for various times

TEM images in the grain of as-solution-annealed and as-aged Alloy 617 plate are shown in Figure 13. Though little or no precipitate was observed in the as-solution-annealed material, fine γ ' phases in the grain were observed in the as-aged material.

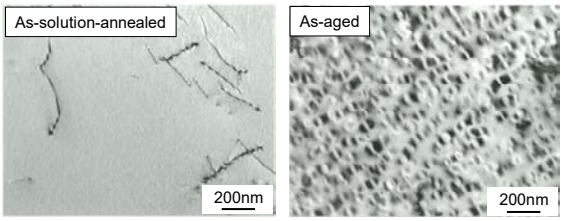

Figure 13 TEM images in grain of as-solution-annealed and as-aged Alloy 617

Figure 14 shows the calculated volume fraction of γ' phase versus time at 700°C, 750°C and 800°C using JMatPro version 8.0. The γ' phase precipitates in the early stages of thermal aging at these temperatures. The γ' phase reached equilibrium volume after 10 hours of heating at 700°C. Figure 15 shows changes in Vickers hardness in the grain near the edge of the specimens before and after the test with holding times of 3 hours and 300 hours or more for as-solution-annealed specimens, as-aged specimens and simulated HAZ specimens of aged material. Hardness of the as-aged specimens before and after three-point bending testing, except for specimens after the test with holding time of 300 hours, were much higher than that of the as-solution-annealed materials and simulated HAZ materials due to the difference of the amount of γ' phase. The hardness of as-solution-annealed and simulated HAZ specimens after the test with a holding time of 300 hours increased to almost the same hardness of aged material after 508 hours of testing due to precipitation hardening. The hardness of simulated HAZ specimens before the test was almost the same as that of solution annealed material. This indicates that γ ' phase dissolved in the matrix due to the grain coarsening heat treatment. Thus, susceptibility to high stress relaxation cracking was caused by γ' phase strengthening in the grains as opposed to that of the grain boundary. However, it was assumed that additional factors promoted the susceptibility to stress relaxation cracking since the γ' phase fraction of solution-annealed materials reached equilibrium volume at an early stage of thermal aging as shown in Fig.14.

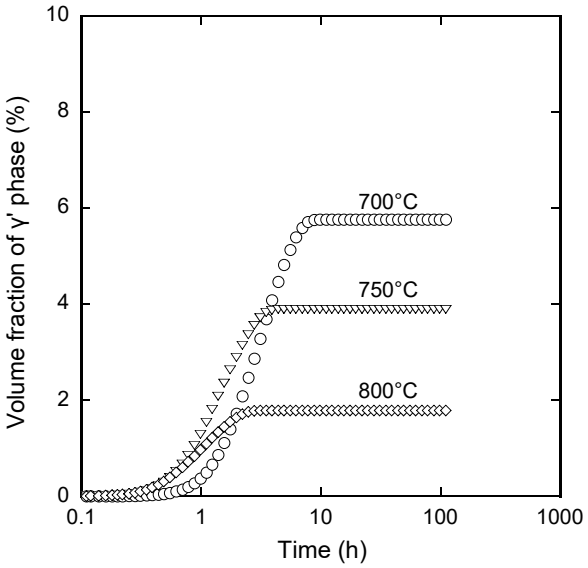

Figure 14 Calculated volume fraction of gamma prime phase with temperature for Alloy 617 using JMatPro version 8.0

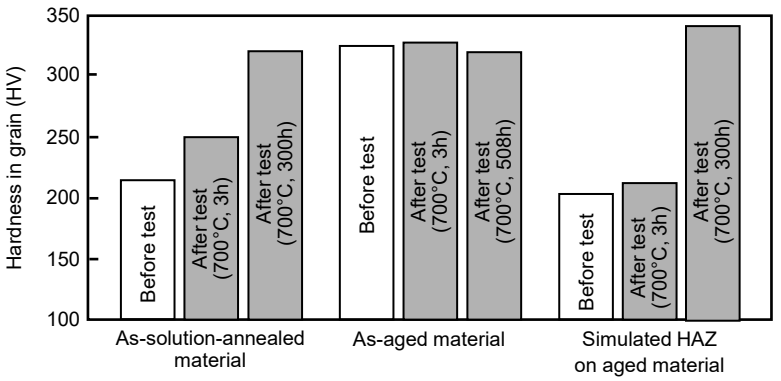

Figure 15 Vickers hardness changes in the grain near the edge of specimens before and after three-point bending test

The yield stress of aged material was increased by precipitation hardening as shown in Fig.4. In this case, since the residual stress with the initial strain of aged material was two times higher than that of the solution-annealed material, the creep strain during three-point bending testing also increased. In addition, since grain boundary carbides existed initially in the aged material, ductility in the grain boundary was assumed to be low. Therefore, the creep strain accumulates at the grain boundaries due to relative weakening compared to within the grains strengthened by γ' phase. When creep strain during the test exceeded the ductility limit in the grain boundary, it was assumed that cracking initiated intergranularly and progressed.

Quantitative evaluation results of stress relaxation cracking susceptibility for Alloy 617

Figure 16 presents the relationship between initial strain and creep strain with stress relaxation during the three-point bending tests, which were calculated by FEA of as-aged Alloy 617 plates. According to these results, it was observed that aged Alloy 617 has a risk of stress relaxation cracking in the high initial strain region exceeding the critical strain curve. Critical creep strain tends to decrease with increased initial strain. Regarding the uniaxial creep test results, reduction

of creep ductility was confirmed in cold-formed materials [12-14]. When the initial strain is large, plastic deformation volume will also become large, resulting in a reduction of creep ductility. Accordingly, it is considered that deterioration in critical strain will occur in highly and initially strained materials. The critical conditions that cause cracks could be estimated from the stress relaxation cracking boundary from the relationship between the initial strain and the creep strain during the three-point bending testing.

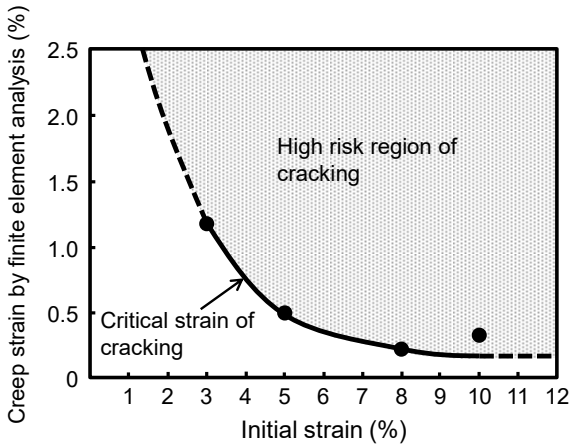

Figure 16 Relationship between creep strain and initial strain of as-aged Alloy 617 plate

CONCLUSION

The weld cracking susceptibility of A-USC candidate Ni-based alloys and stress relaxation cracking susceptibility of Alloy 617 were evaluated. The following results were observed.

1) Solidification cracking susceptibility of Alloy 617 was the highest; followed by HR35, Alloy 740 and Alloy 141, which were high; and then by HR6W and Alloy 263, which were relatively low. In addition, liquation cracking was observed in the HAZ of Alloy 617.

2) The reheat cracking susceptibilities of Alloy 617, Alloy 263, Alloy 740 and Alloy 141 were somewhat higher than those of HR6W and HR35, which have good creep ductility due to the absence of γ' phase precipitates. From the stress relaxation test results, it was determined that the post welding heat treatment of candidate A-USC alloys be 900°C or higher. Furthermore, it was considered desirable for alloys with a large volume fraction of the γ' phase, such as Alloy 740 and Alloy 141, to be subjected to heat treatment at 980°C or higher.

3) An evaluation method for stress relaxation cracking susceptibility was developed by applying a three-point bending test using a specimen with a V-notch, and the susceptibility of stress relaxation cracking for aged Alloy 617 was experimentally replicated. It was proposed that a greater magnitude of creep strain occurs via stress relaxation during the three-point bending test due to higher yield strength caused by γ' phase strengthening, and low ductility due to grain boundary carbides promoting stress relaxation cracking. The critical cracking region could be estimated from the relationship between the initial strain and creep strain during three-point bending testing of as-aged Alloy 617.

ACKNOWLEDGMENT

A part of this work was based on results obtained in a project subsidized by the Ministry of Economy, Trade and Industry and the New Energy and Industrial Technology Development Organization (NEDO) of Japan.

REFERENCES

[1] David, S.A., Siefert, J.A., DuPont, J.N. and Shingledecker, J.P., "Weldability and weld performance of candidate nickel base superalloys for advanced ultrasupercritical fossil power plants part Ⅰ : fundamentals", Science and Technology of Welding and Joining, Vol. 20, No.7 (2015), pp. 532-552.

[2] Siefert, J.A., Shingledecker, J.P., Dupont, J.N. and David, S.A., "Weldability and weld performance of candidate nickel base superalloys for advanced ultrasupercritical fossil power plants part II: weldability and cross-weld creep performance", Science and Technology of Welding and Joining, Vol.21, No.5 (2016), pp.397-428

[3] Suzuki, M., Maruyama, T., Nanba S. and Takeda, H., "Research for the Quantitative Evaluation of Solidification Cracking Susceptibilities in Ni-base Alloy Weld Metals", KOBE STEEL ENGINEERING REPORTS, Vol.54, No.2 (2004), pp.43-46.

[4] Okada, K., Igarashi, M., Ogawa K., and Matsuo H., "Sensitivity of Reheat Cracking on Austenitic Stainless Steel Containing Nb", Vol.17 (2004), pp.928.

[5] Fukuda, M., Yoshida, T., Iseda, A., Semba, H., Saito, E., Kitamura, M., Dohi, T., Fukutomi, H., Sato, K., Takahashi, K., Saito, N., Hirakawa, Y., Nishii, T., Takahashi, T., Takano, T., Matsubara, Y. and Yagi, Y., "700°C A-USC technology development in Japan", *Proc. 8th* Int. Conf. on Advances in Materials Technology for Fossil Power Plants, Albufeira, Algarve, Oct. 2016, pp. 12–23.

[6] Directorate-General for Research and Innovation (European Commission), Component test facility for a 700°C power plant (Comtes700). https://publications.europa.eu/en/publication-detail/-/publication/655f4dba-f07a-49c7-9033-91197f01a3aa/language-en/, 2013 (accessed 15 March 2018).

[7] Sunders, N., Miodownik, A.P. and Schille, J.-PH., "Modelling of the thermo-physical and physical properties for solidification of Ni-based superalloys", Journal of Materials Science, Vol.39, Issue 24 (2004), pp.7237-7243

[8] SPECIAL METALS, INCONEL® alloy 617. http://www.specialmetals.com/assets/smc/documents/alloys/inconel/inconel-alloy-617.pdf/, 2005 (accessed 15 March 2018).

[9] Matsuda, F., "Hot Tearing and its Dependability on Alloying Elements in Weld Metal during Solidification", Journal of the Japan Welding Society, Vol.36, No.9 (1967), pp.973-986

[10] Ernst, S. C., 'Weldability studies of Haynes 230 alloy', Welding Journal, Vol.73, (1994), pp.80-s-89-s

[11] Semba, H., Okada, H. and Igarashi, M., " Creep properties and strengthening mechanisms in 23Cr-45Ni-7W (HR6W) alloy and Ni-base superalloys for 700°C A-USC boilers", *Proc. 5th* Int. Conf. on Advances in Materials Technology for Fossil Power Plants, Marco Island, FL, Oct. 2007, pp.168-184

[12] Saito, N., Komai, N., Hashimoto, K. and Kitamura, M., "Long-term creep rupture properties and microstructures in HR6W (44Ni-23r-7W) for A-USC boilers", *Proc. 8th* Int. Conf. on Advances in Materials Technology for Fossil Power Plants, Albufeira, Algarve, Oct. 2016, pp.419-429.

[13] Shioda, Y., Kubushiro, K., Sakakibara, Y., Nomura, K. and Murata, Y., "The effect of cold working on creep rupture strength and microstructure of Ni-23Cr-7W Alloy", International Journal of Materials Science and Applications, Vol.6, No.4 (2017), pp.178-189.

[14] Kubushiro, K., Shiota, Y. and Nomura, K., "Effect of pre-strain on the creep strength of Ni-based Alloys for A-USC boilers", Transactions of the Indian Institute of Metals, Vol.70, Issue 5 (2017), pp.1261-1268.